INTERNATIONAL JOURNAL FOR NUMERICAL METHODS IN FLUIDS
Int. J. Numer. Meth. Fluids 2004; **44**:431–446 (DOI: 10.1002/fld.653)

A numerical and experimental investigation of the interactions between a non-uniform planar array of incompressible free jets

C. H. Isaac Manohar[1], T. Sundararajan[2], V. Ramjee[1,*,†] and S. Sasi Kumar[1]

[1]*Department of Applied Mechanics, IIT Madras, Chennai 36, India*
[2]*Department of Mechanical Engineering, IIT Madras, Chennai 36, India*

SUMMARY

The interaction between multiple incompressible air jets has been studied numerically and experimentally. The numerical predictions have been first validated using experimental data for a single jet configuration. The spreading features of five unequal jets in the configuration of one larger central jet surrounded by four smaller equi-distant jets, have been studied, for different lateral spacing ratios of 1.5, 2.0 and 2.5 and a central jet Reynolds number of 1.24×10^5 (corresponding to a Mach number of 0.16). Flow of five equal jets has also been simulated, for the sake of comparison. The jet interactions commence at an axial distance of about 3–4 diameters and complete by an axial distance of about 10 diameters for the lowest spacing ratio of 1.5. For larger spacing ratios, the length required for the start and completion of jet interaction increase. Peripheral jets bend more towards the central jet and merge at a smaller distance, when their sizes are smaller than that of the central jet. The entrainment ratio for multiple jets is higher than that for a single jet. Excellent agreement is observed between the experimental data and theoretical predictions for both mean flow field and turbulent quantities, at regions away from the jet inlet. The potential core length and initial jet development, however, are not predicted very accurately due to differences in the assumed and actual velocity profiles at the jet inlet.

KEY WORDS: jets; entrainment; bending; turbulent shear stress; turbulent kinetic energy

1. INTRODUCTION

Jets are encountered in many practical applications such as civil and military aircrafts, rocket nozzle thrust vectoring devices, V/STOL aircraft, air curtains etc. In most combustion devices, fuel and oxidizer streams mix with each other in the form of subsonic jets. In these applications, important parameters such as thrust developed and combustion efficiency depend on the jet spreading characteristics.

*Correspondence to: V. Ramjee, Department of Applied Mechanics, Indian Institute of Technology—Madras, Chennai 600 036, India.
†E-mail: vramjee123@hotmail.com

Received 17 April 2002
Revised 17 May 2003

Active and passive methods of jet flow control have been widely employed to achieve the desired spreading features of jets and to reduce the level of noise emanating from them. Some of the popular methods employed for jet flow control are acoustic forcing, placement of tabs at nozzle exit and use of non-circular nozzles or multiple jet configurations.

Wygnanski and Fiedler [1] performed a comprehensive study of the self-similar region of a round jet and reported detailed data on the moments, intermittency, microscales and integral scales. Donaldson and Snedeker [2] studied the structure of a compressible free jet and also the decay of subsonic jets issuing from round nozzles into a quiescent atmosphere. Crow and Champagne [3] showed that using acoustic input at 2% of the exit speed and at a Strouhal number (fD/U_e) of 0.3, the axial turbulent intensity measured along the centreline of the jet attains its peak value at four diameters from the exit of the nozzle. The entrained volume flow increases by 32% over the unforced case. Zaman and Hussain [4] have shown suppression of turbulence, by acoustic excitation at $St_{\theta_e} = 0.017$ (fD/U_e) where θ_e is the momentum thickness of the boundary layer in the nozzle exit plane. The spreading rate of an elliptic jet is quite different from that of a circular jet. The major and minor axes switch over. Acoustic excitation moves the switch over location upstream [5]. The preferred mode occurs at $St_D = 0.4(fD/U_e)$ where the equivalent diameter is given by $D = 2(ab)^{1/2}$ and a, b are the semi-major and semi-minor axes. Elbana and Sabbagh [6] showed that in the case of two non-equal plane parallel jets, the axis of the combined jet shifts closer to the power jet as the velocity of the weaker jet decreases. Ho and Gutmark [7] and Hussain and Hussain [8] showed that the overall spreading of small aspect ratio elliptic jets is clearly more than that of an axisymmetric jet. Gutmark and Grinstein [9] presented an elaborate review of the passive control methods employed in the past. Zaman [10] showed that the flow induced by the pair of streamwise vortices generated by placing tabs at the edge of a rectangular nozzle can effectively enhance or suppress axis switching. Zaman [11] studied the comparative spreading characteristics of free jets from a set of asymmetric and axisymmetric nozzles. Tabs at the exit of rectangular and round jet nozzles increase the spreading rates of incompressible and compressible jets.

Verma and Rathakrishnan [12] experimentally studied the characteristics of small aspect ratio elliptic jets and the influence of notches in the minor axis. It was seen that notches cause enhanced mixing close to the orifice exit. Lau *et al.* [13] carried out measurements of velocity for subsonic and supersonic free jets issuing into atmosphere, using a laser velocimeter. These measurements indicated a reduction in the spreading rate of mixing layer with increasing Mach number and a corresponding increase in the length of the potential core.

Krothapalli *et al.* [14] conducted experiments on multiple jet configurations and studied the modified structure of a rectangular jet in such configurations. The results were presented for incompressible jets only. Nozzles were placed in a row-structure (side by side) and the resultant jet flow features were studied. Raghunathan and Reid [15] showed that improved mixing in the case of multiple jets results in a rapid decrease in peak velocities and a multiple jet nozzle with five-jets is advantageous for noise reduction without significant reduction in the momentum.

The above literature survey reveals that a majority of the available studies are experimental in nature and that there is a dearth of detailed numerical simulations. In particular, there is a strong need to investigate the spreading features of multiple jets. In the present study, experimental and numerical investigations have been performed on the interaction between five incompressible jets, in the configuration of a large central jet surrounded by four

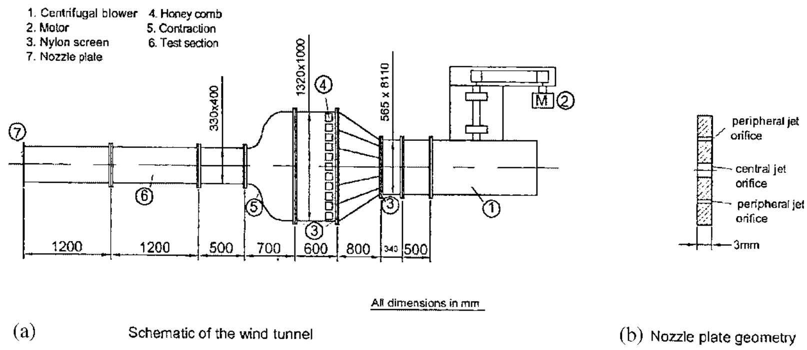

Figure 1. Experimental set-up: (a) schematic of the wind tunnel; and (b) nozzle plate geometry.

smaller peripheral jets. Five equal jets have also been simulated theoretically, for the sake of comparison.

2. EXPERIMENTAL STUDY

Experiments on five jet flow configurations have been performed using a wind tunnel with a test section of $0.4\,\mathrm{m} \times 0.33\,\mathrm{m}$ size, as shown in Figure 1(a). A 20 hp blower with a maximum air flow rate of $5\,\mathrm{m}^3/\mathrm{s}$ and head of 200 mm water, is employed. An aluminum plate of 3-mm thickness is fixed at the end of the wind tunnel and in this plate suitable holes are made for the jet flow as shown in Figure 1(b). The flow geometry with a central jet of 30 mm diameter (D) and four peripheral jets of 15 mm diameter is shown in Figure 2. The nozzle spacing between the axes of the central and peripheral jets is varied as 45, 60 and 75 mm so that the spacing ratio values of $S/D = 1.5$, 2.0 and 2.5 are obtained. The Reynolds number of flow based on the diameter and inlet velocity of the central jet is 1.24×10^5. A Pitot tube of 1 mm OD is used to measure the total pressure at different locations in the jet.

The total pressure was measured using the Prandtl type manometer with a least count of 0.1mm of H_2O. Since the smallest values of dynamic pressure head measured in the experiment was 5 mm H_2O, the maximum estimated error for the total pressure is $\mathrm{d}p/p = \mathrm{d}h/h \leqslant 0.1/5 = 2\%$. The flow velocity ($u$) being proportional to $\sqrt{h}$, the estimated maximum error for the velocity measurement, $\mathrm{d}u/u \leqslant 1\%$. Repeated measurements also showed that the velocity data were reproducible within a scatter of $\pm 3\%$.

3. NUMERICAL SIMULATION OF SINGLE AND MULTIPLE JET FLOW

Jet flow features have been simulated with the help of FLUENT 5.5 software, by numerically solving the turbulent incompressible Navier–Stokes equations. A non-uniform structured mesh based solver using the Finite volume method has been invoked. The standard k–ε turbulence model has been employed for obtaining the eddy viscosity at each location. For the five-jet configuration, one-quarter geometry has been considered (Figure 2(b))

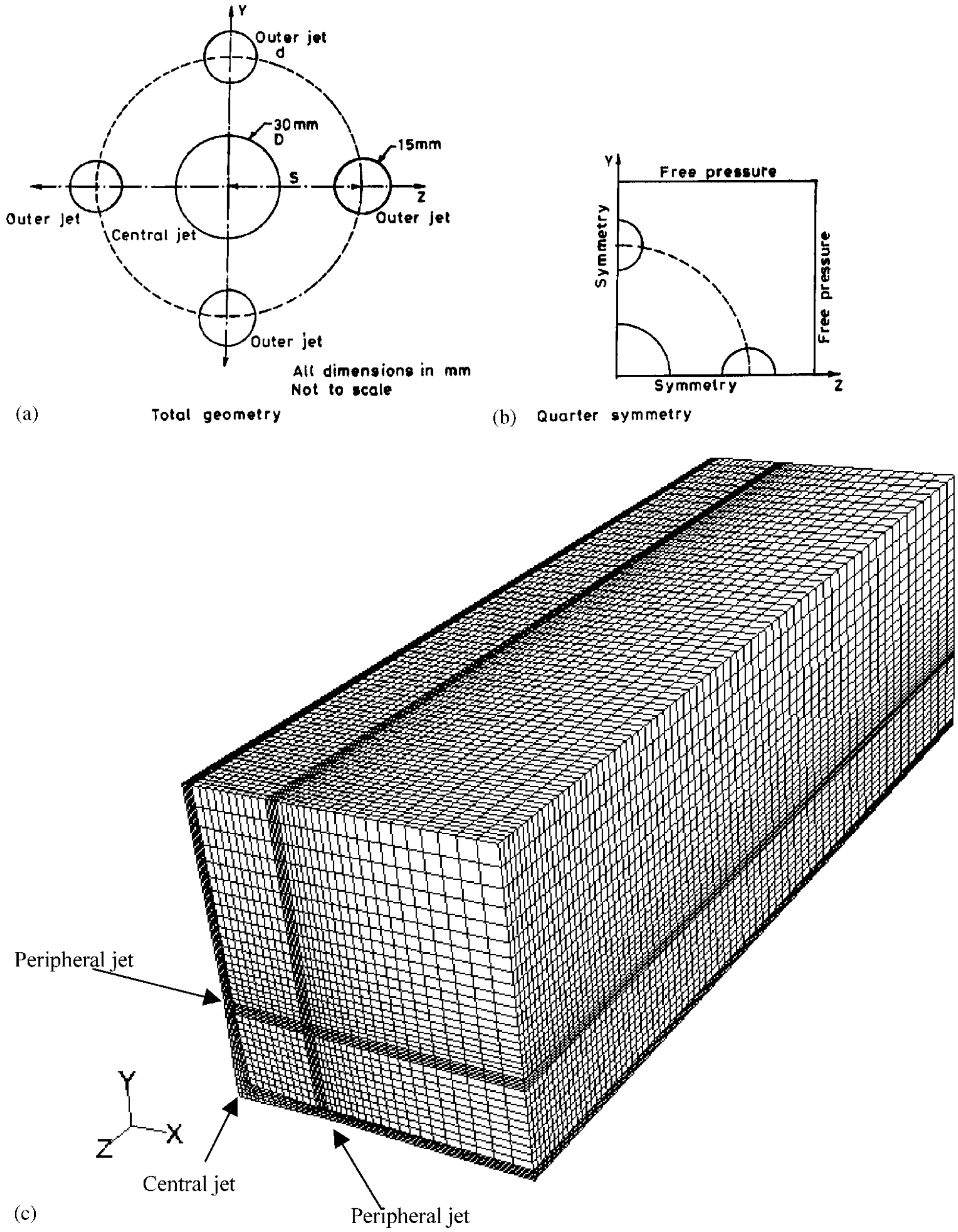

Figure 2. Geometric arrangement of nozzles: (a) total geometry; (b) quarter symmetry; and (c) schematic grid used for multiple jet simulation.

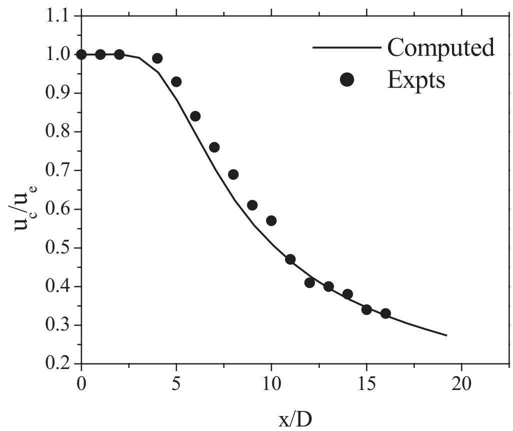

Figure 3. Comparison of the computed and experimental results of the present study for the centreline velocity variation in a single jet.

due to symmetry of the flow situation [16]. (Vijayakumar studied a similar configuration in supersonic flow.) A schematic of the structured grid used for the geometry is shown in Figure 2(c).

Boundary conditions employed for the simulation are listed below.

Inflow (jet inlet): $u = u_0$; $v = 0.0$

Outflow: The velocity components of u and v are determined from the interior domain by extrapolation. The static pressure is set equal to the ambient pressure p_∞. The outflow boundary is located at a distance of 100 nozzle diameters.

Symmetry plane: The normal velocity is set as zero and normal derivatives of all flow quantities are zero.

Body surface: No slip condition for velocity components is imposed $(u = v = 0)$ on the common end wall in which the jet nozzles are located.

The convergence criterion applied is the sum of normalized residue for the variables of mass, velocity components and turbulence quantities k, ε being equal to 1×10^{-5}.

4. RESULTS AND DISCUSSION

4.1. Validation for single jet flow

Figure 3 shows the centreline velocity variation in a single jet and the numerical and experimental results compared in the figure agree very well with each other. Grid independence was achieved for a mesh of 150×75 divisions in the axial and radial directions respectively, for the results presented here. The axial variations of jet half-width and volume flow rate are shown in Figures 4(a) and 4(b). Typical radial profiles of turbulent kinetic energy and Reynolds stress are shown in Figures 5(a) and 5(b). The figures also illustrate that the numerical predictions compare very well with the corresponding experimental data reported in literature or obtained in this study.

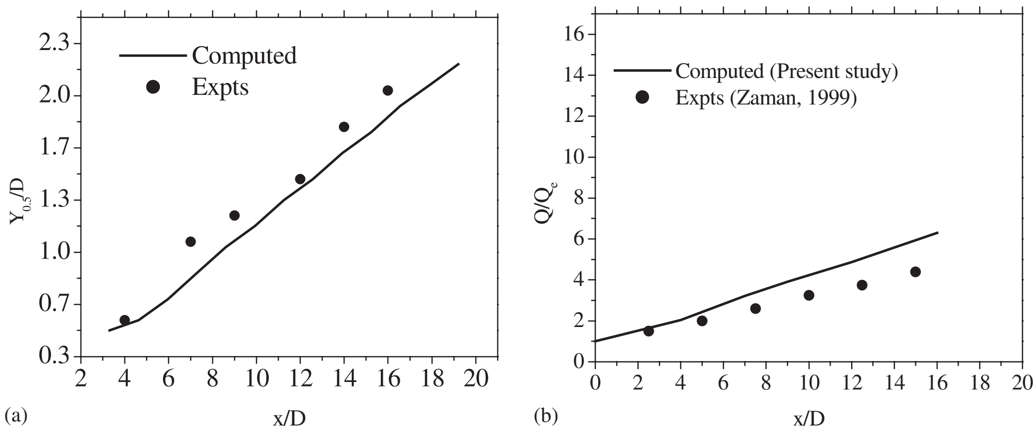

Figure 4. (a) Comparison of present computed and experimental results for the half-width variation in a single jet; and (b) variation of volume flow rates for single jet.

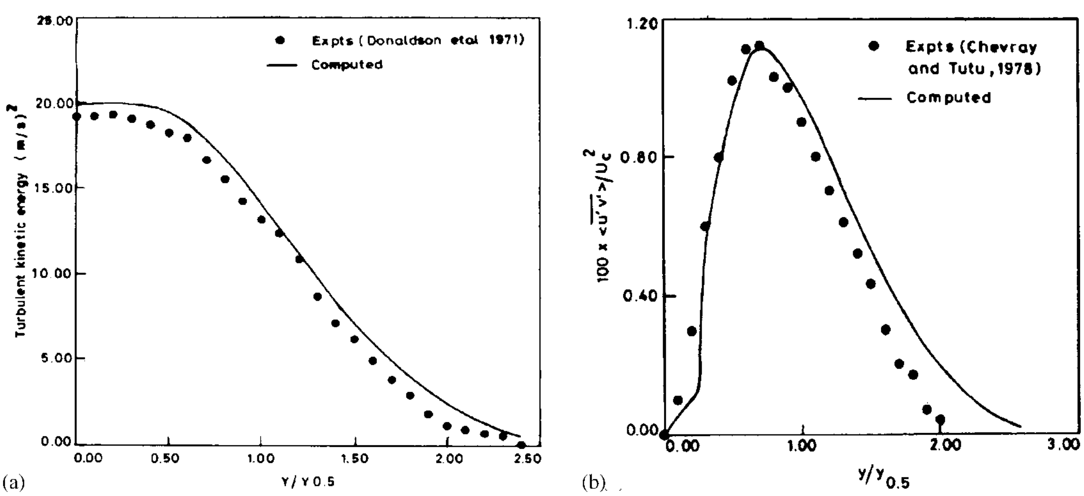

Figure 5. (a) Variation of turbulent kinetic energy in a single jet; and (b) variation of Reynolds shear stress in a single jet.

4.2. Results for five jets

In order to test the grid independence of the predicted solutions, grids with $71 \times 41 \times 41$, $101 \times 41 \times 41$, $71 \times 61 \times 61$ nodes have been employed. Here, the first dimension gives the number of cells in the axial direction and the second and third dimensions represent the number of cells in the lateral directions. In all the cases, the diameter of the larger jet (D) is used as the normalizing scale for length in all directions.

The prediction of centreline velocity profile is shown in Figure 6. It does not show marked variations for the grids employed, even though the total number of nodes employed in each grid is significantly different. Hence, a grid of $71 \times 41 \times 41$ has been used for all further

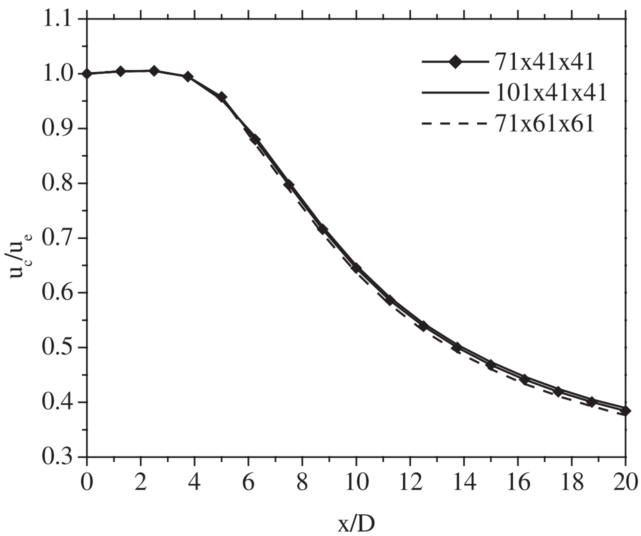

Figure 6. Grid independence study for five-jet configuration.

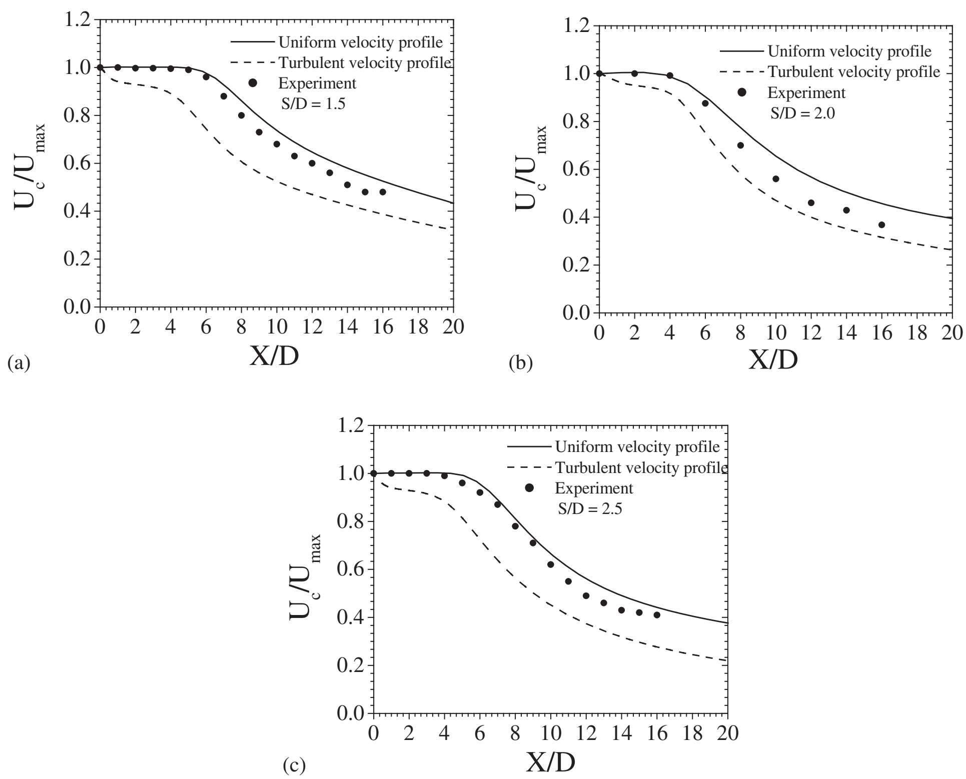

Figure 7. Comparison of centreline velocities for five unequal jet configuration ($d/D = 0.5$).

computations. Grid points are clustered in such a way that the steep gradients existing near the nozzle exit and jet boundaries are captured accurately.

Simulations for the flow of a larger central jet surrounded by four equi-distant smaller jets have been carried out for the central jet Reynolds number of 1.24×10^5 and spacing ratios of 1.5, 2.0 and 2.5. The results are presented in the form of mean velocity profiles at different axial locations and centreline variations for various flow quantities in the axial direction.

The mean velocity variation along the axis of the central jet is shown in Figure 7 for different spacing ratios. As the spacing ratio increases, the decay of the central jet is greater due to a reduction in the momentum exchanged with the side jets. Some minor deviations are observed between the experimental and computational results, due to the fact that the length of the potential core (distance up to which $u/u_e \cong 1$) sensitively depends on the inlet velocity profile, turbulence model used in numerical simulation and the shape and finish of the nozzles employed in experiment. Infact, repeating the computational simulation for different inlet profiles corresponding to uniform inlet velocity and fully developed turbulent profile inside a circular duct, showed that the present experimental results lie between the predictions for the uniform and the fully turbulent cases. This is to be expected because in a short orifice, flow development is not complete. Not withstanding the differences between the experimental condition and the assumed input condition for the numerical simulation, reasonable agreement is observed between both sets of results. The predicted pressure contours (gauge values) for different lateral nozzle spacings are shown in Figure 8. It is clear from these figures that a low pressure region occurs due to entrainment of the fluid between the jets. The variation of pressure in the lateral direction across the peripheral jets causes bending of these jets towards the central jet. The minimum pressure decreases as the nozzle spacing increases, thereby causing a greater bending of the side jets towards the central jet. However, the region of low pressure extends further in the axial direction for a larger spacing. This causes an increase in the merger length for the jets, as discussed subsequently. The predicted radial velocity profiles at various axial locations beyond the potential core region are shown in Figures 9 and 10, and they are also compared with corresponding experimental data obtained in the present study. Separate velocity peaks are seen for the peripheral and central jets for smaller axial distances. After some distance from the nozzle exit plane, the peripheral jet is seen to merge with the central jet. A careful examination of the peak velocity location for the peripheral jet indicates that the jet axis bends towards the central jet. This bending of the peripheral jet can be attributed to the asymmetry in air-entrainment which induces lateral movement. From a comparison of the results shown in Figures 9 and 10, it is evident that the merger distance between the peripheral and central jets increases with spacing ratio. The figures also illustrate that the agreement between the experimental and computed results for the radial profile of mean velocity is reasonably good in all the cases compared.

In order to understand the effects of relative jet size on mixing phenomena, computational studies have also been carried out for five equal jets under the same flow conditions and spacing ratios, as in the previous cases. The radial profiles of mean axial velocity shown in Figures 11 and 12 indicate that the general shapes of the profiles are similar for both equal and unequal jets at various axial locations. However, the decay of the peripheral jet is slower and hence, merger between the central and peripheral jets occurs at a larger axial distance. It is evident that the bending of peripheral jet towards the central jet is less for the equal jet case. As seen earlier for the unequal jets, the merger distance increases with nozzle spacing for the equal jets also.

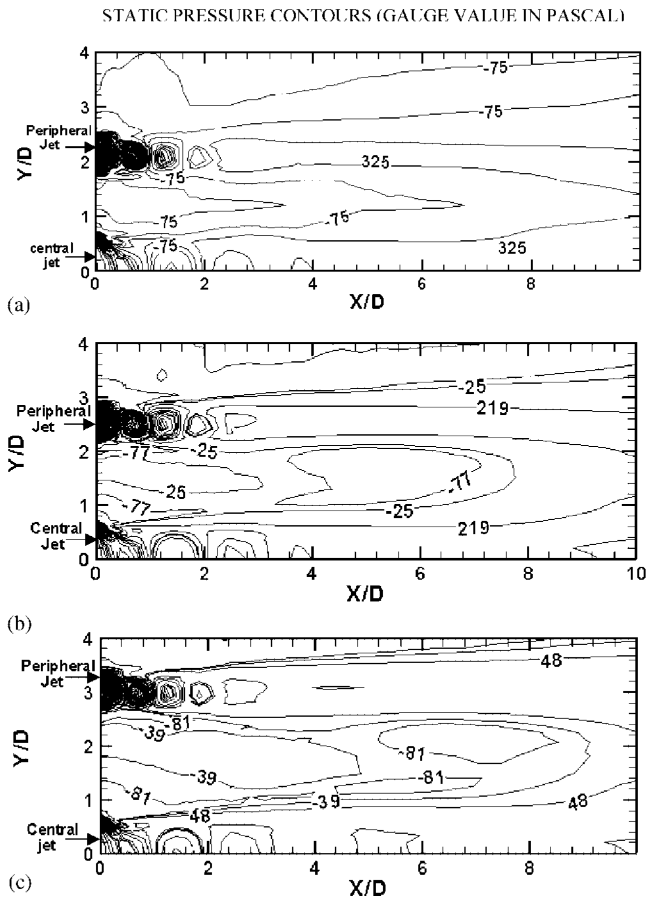

Figure 8. Comparison of static pressure contours for five unequal jet configuration ($d/D = 0.5$): (a) $S/D = 1.5$; (b) $S/D = 2.0$; and (c) $S/D = 2.5$.

The velocity decay along the axis of the central jet is shown in Figure 13, for the cases of equal and unequal jets. The decay of velocity along the centreline for the unequal jet case is remarkably different from that of the equal jet case. This can be attributed to the facts that there exists a better interaction of the jets in unequal jet case due to greater bending of the peripheral jets and hence better mixing is achieved. The velocity decay of the single jet is greater when compared to those of the unequal and equal jets. The length of the potential core of the single jet is also less as compared to the other two configurations. Evidently, exchange of momentum with the side jets decreases the decay rate and the length of the potential core for the central jet.

In Figure 14, a comparison of the volume flow rate across the jets has been presented for the unequal jets. The volume flow rate has been scaled here by the inlet flow rate of the central jet. For the sake of comparison, the single jet case is also included in the figure. It is evident that the volume flow rate increases in a linear fashion with axial distance, especially for larger axial distances, for both five-jet and single-jet cases. The five-jet configuration

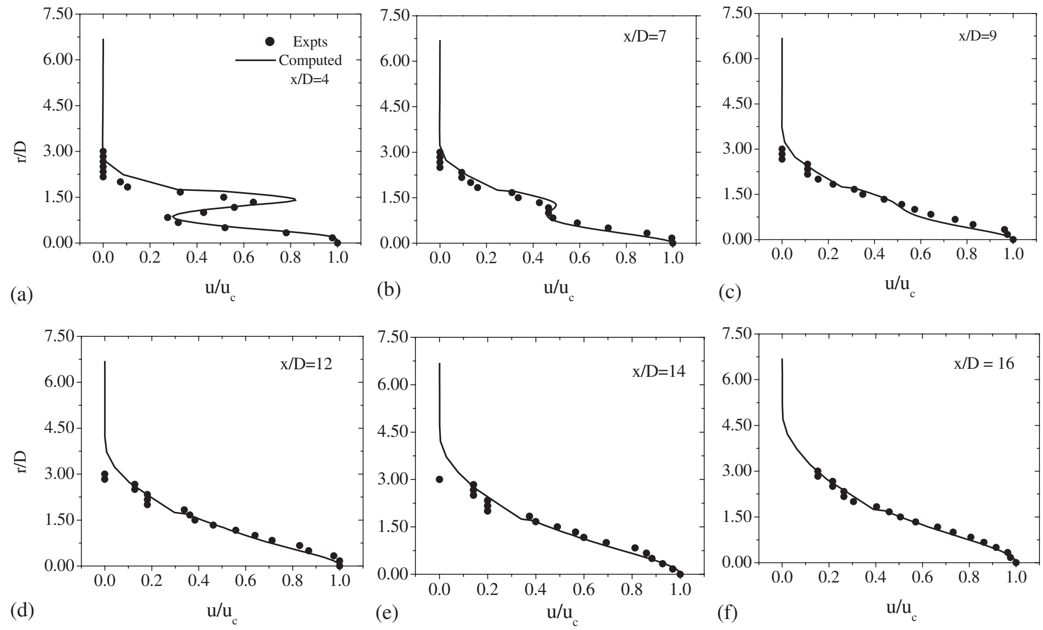

Figure 9. Comparison of mean velocities for five unequal jet configuration ($S/D = 1.5$ and $d/D = 0.5$).

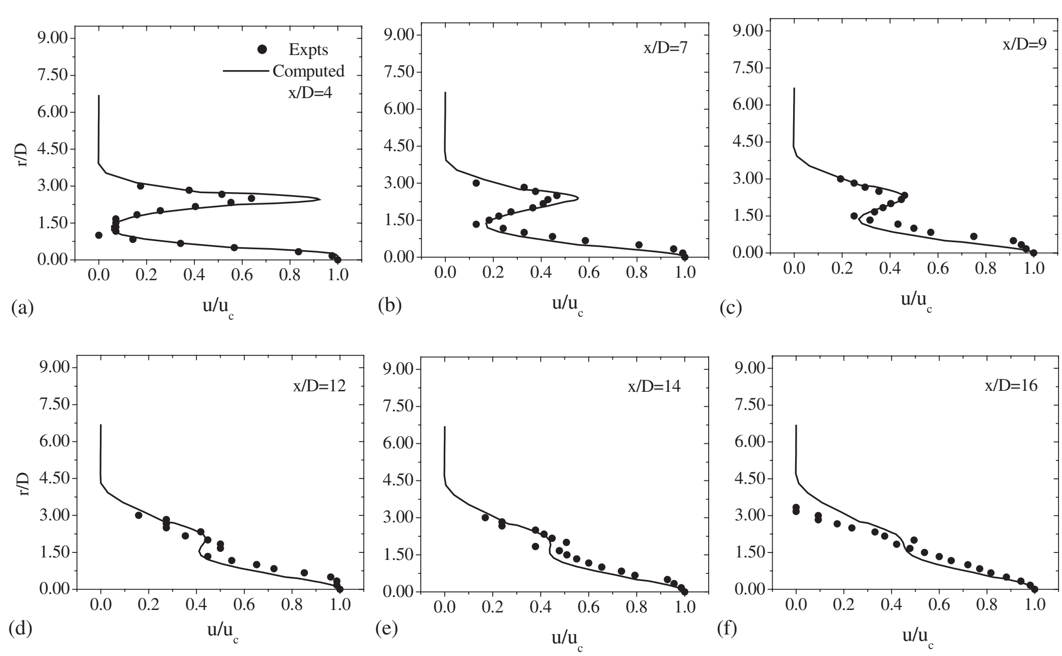

Figure 10. Comparison of mean velocities for five unequal jet configuration ($S/D = 2.5$ and $d/D = 0.5$).

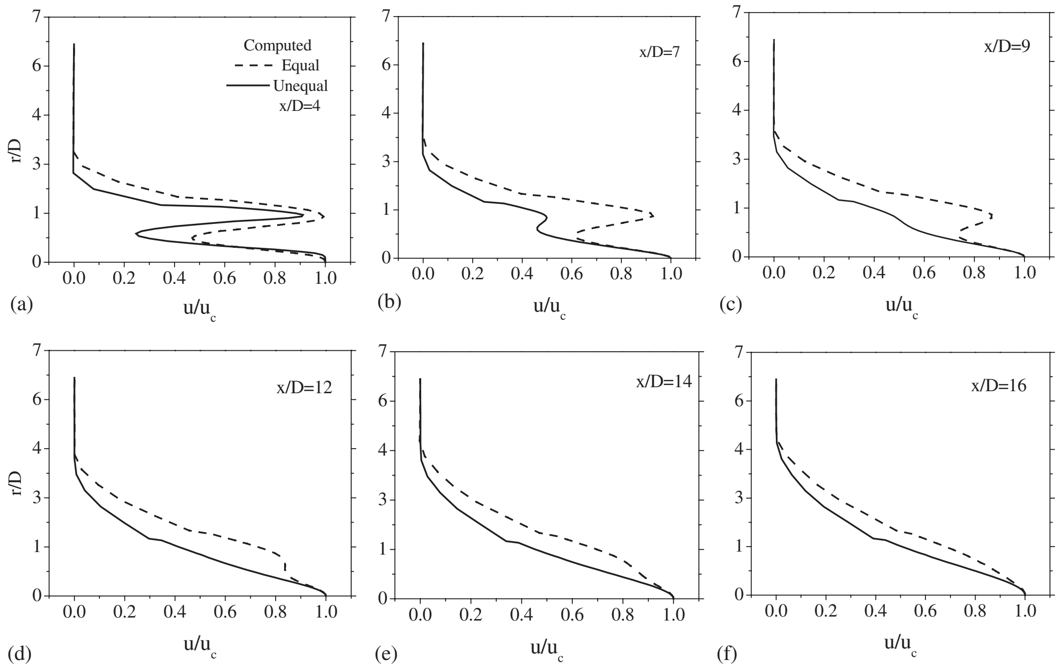

Figure 11. Comparison of mean velocity profiles for five of unequal and equal jet configuration ($S/D = 1.5$).

relatively entrains more ambient air than a single jet, especially for larger spacing ratios. This enhancement can be attributed to the larger lateral velocities induced by peripheral jet bending.

In Figures 15–18, radial profiles of turbulent kinetic energy and Reynolds shear stress are plotted at different axial locations. Although the accuracy of predictions for the turbulent quantities may not be as good as the mean flow results, they are still presented here to provide a qualitative idea of the turbulence generation processes in the shear layers of the jets. For the one-quarter geometry considered in the present study, three distinct peaks are seen in the profiles of turbulent kinetic energy and Reynolds stress, at smaller axial distances. The three peaks correspond to the locations of shear layer for the central jet, inner shear layer for the peripheral jet and the outer shear layer for the peripheral jet, respectively. After merger of the peripheral and central jets, a single peak is observed for the turbulent kinetic energy (TKE) as well as Reynolds stress. For TKE, the peak values gradually move from the shear layer region to the axis of the fully developed combined jet. The peak for the Reynolds stress, on the other hand, occurs at a distance slightly away from the axis. This is to be expected because in a fully developed jet flow, Reynolds stress is zero at the axis due to axisymmetry and it is zero in the far stream due to no flow. For a larger nozzle separation distance, the peaks are more separated than in the case of lower S/D value. It is evident that jet merger is delayed in this case. The TKE profiles for the equal and unequal five jet configurations exhibit three distinct peaks, while a single jet has a single peak (in the shear layer region) only. In the unequal jet case, the peripheral jet peaks diminish at a smaller axial distance due

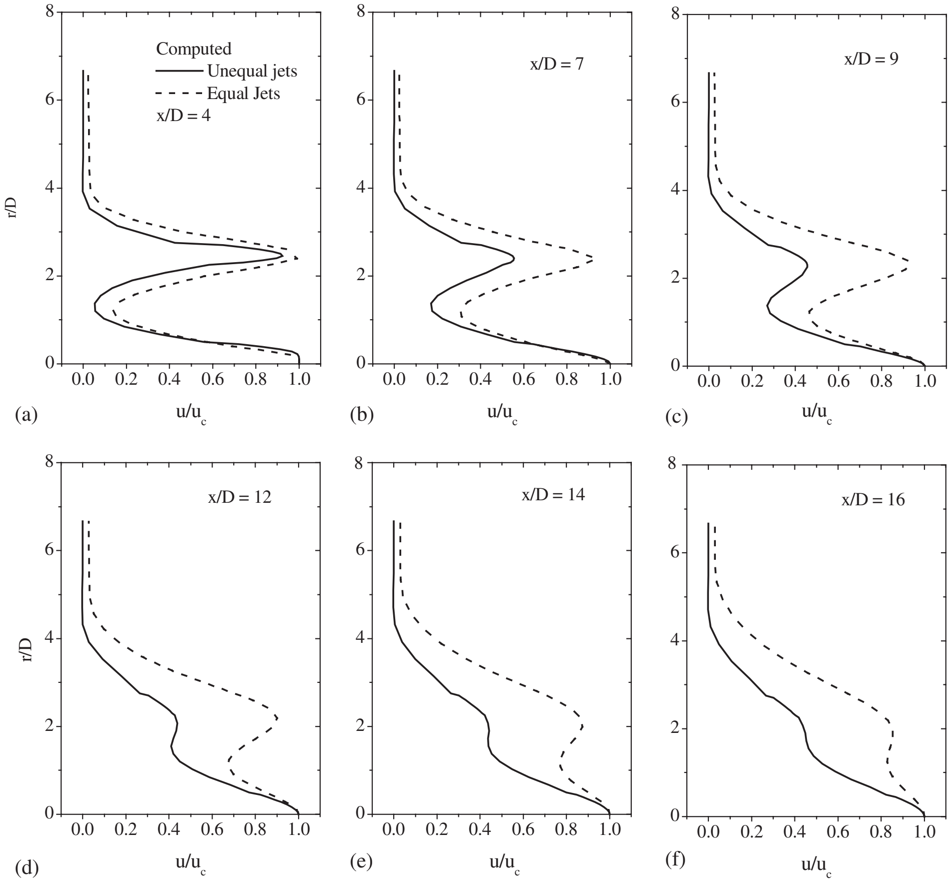

Figure 12. Comparison of mean velocity profiles for five of unequal and equal jet configuration ($S/D = 2.5$).

to merger with the central jet. In the case of equal jets, however, merger of the side jets as well as the development of the combined jet are delayed, as compared to the case of equal jets.

5. CONCLUSIONS

The present study illustrates that the geometry of a multiple jet flow configuration plays a significant role in determining the spread rates of the individual and combined jets, entrainment ratio and the distance for merger of the jets. Excellent agreement is observed between experimental data and theoretical predictions, for both mean flow and turbulent quantities. It is evident that the entrainment ratio for multiple jet configuration is higher than that for a single jet, especially at larger separation distances. Unequal jets interact and merge at smaller axial distances than equal jets, for the same separation ratio (S/D).

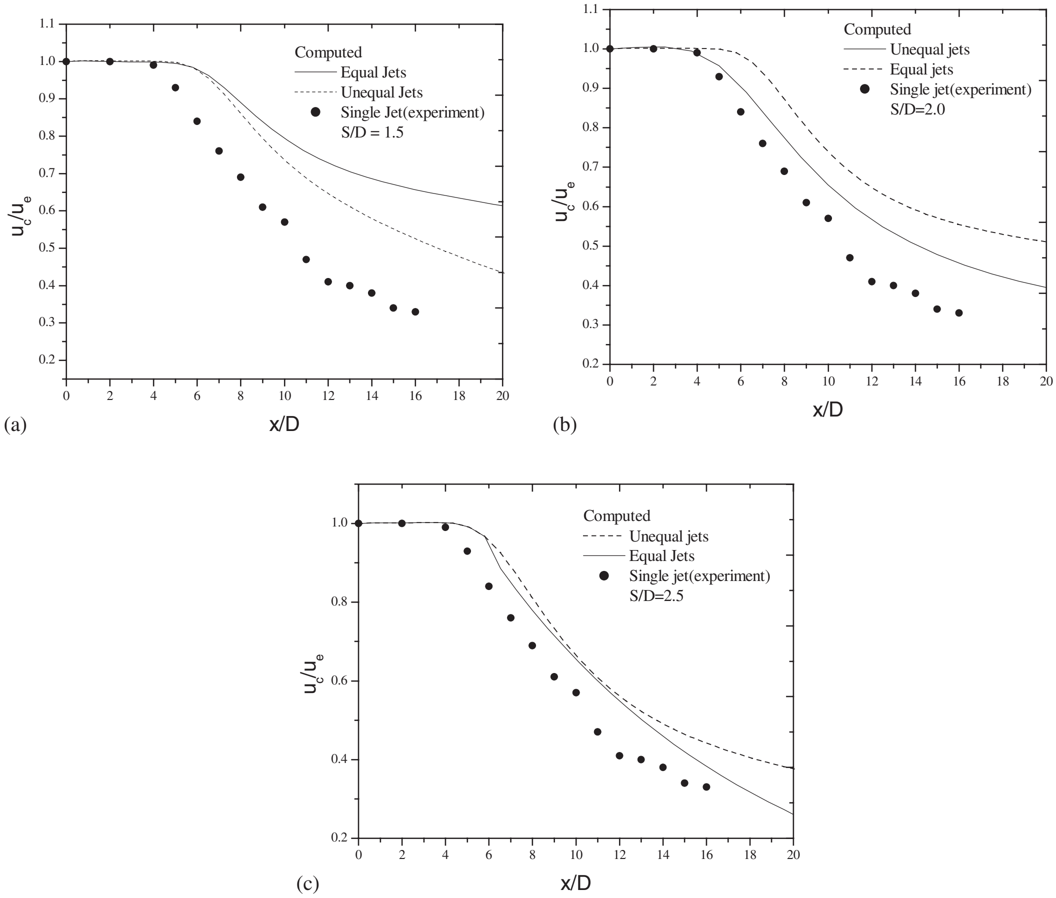

Figure 13. Comparison of the centreline velocity profiles of five equal and unequal jet configurations.

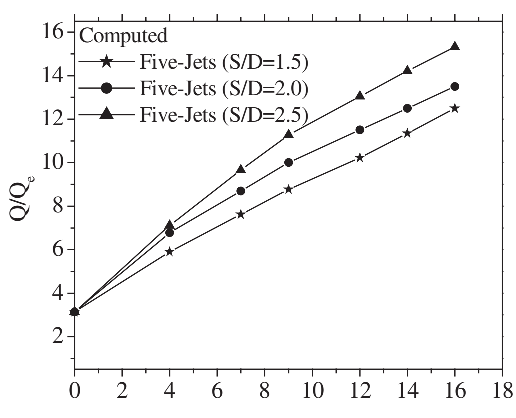

Figure 14. Comparison of volume fluxes of unequal five-jet configuration ($d/D = 0.5$).

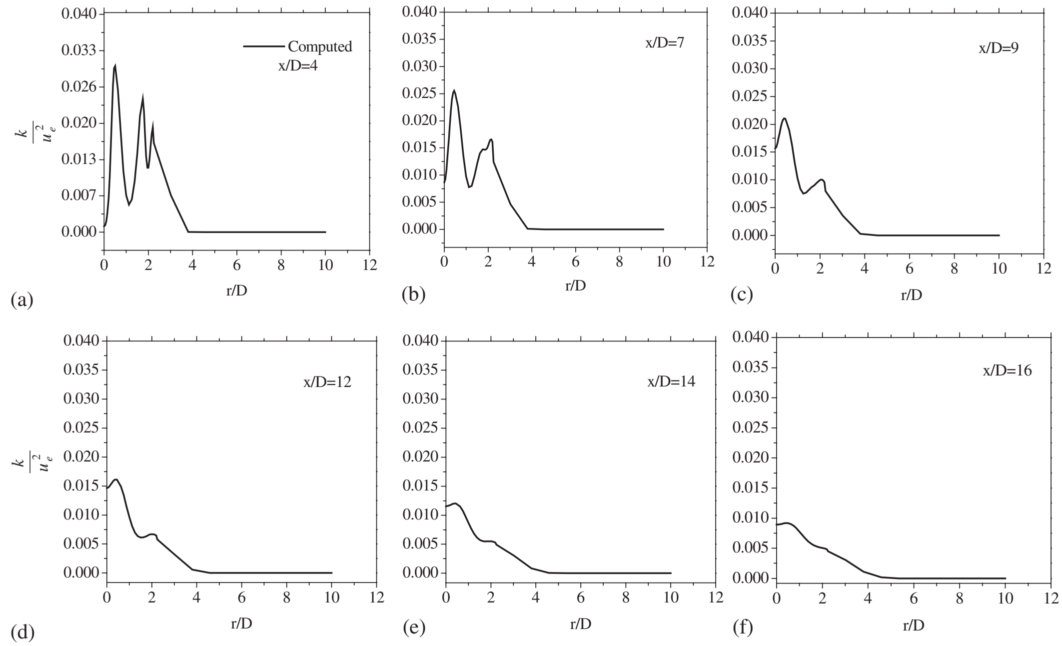

Figure 15. Variation of turbulent kinetic energy for unequal jets ($S/D = 2.0$, $d/D = 0.5$).

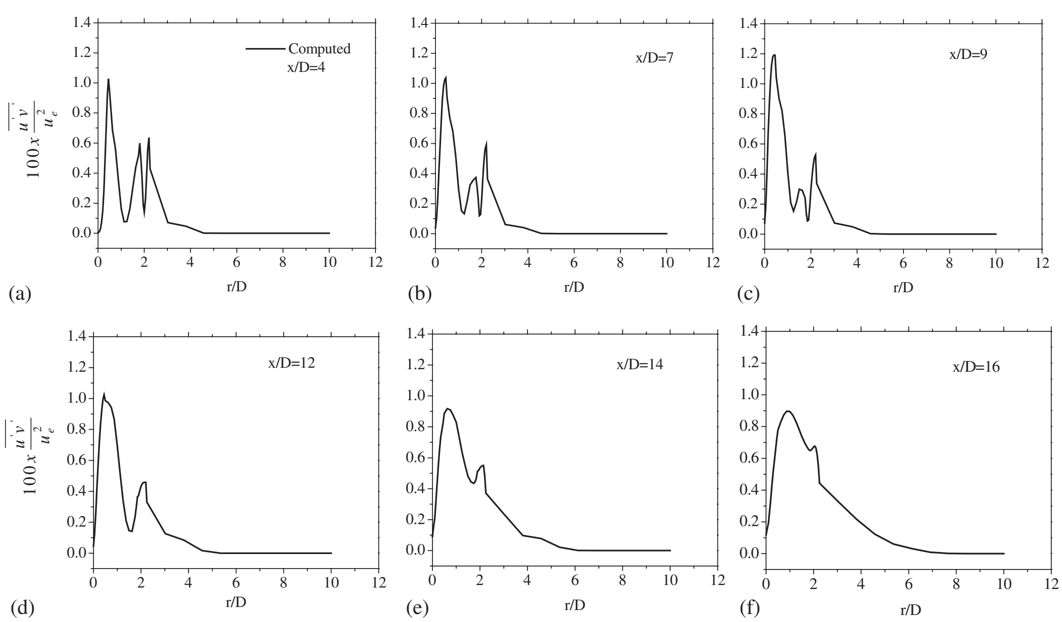

Figure 16. Variation of Reynolds shear stress for unequal jets ($S/D = 2.0$, $d/D = 0.5$).

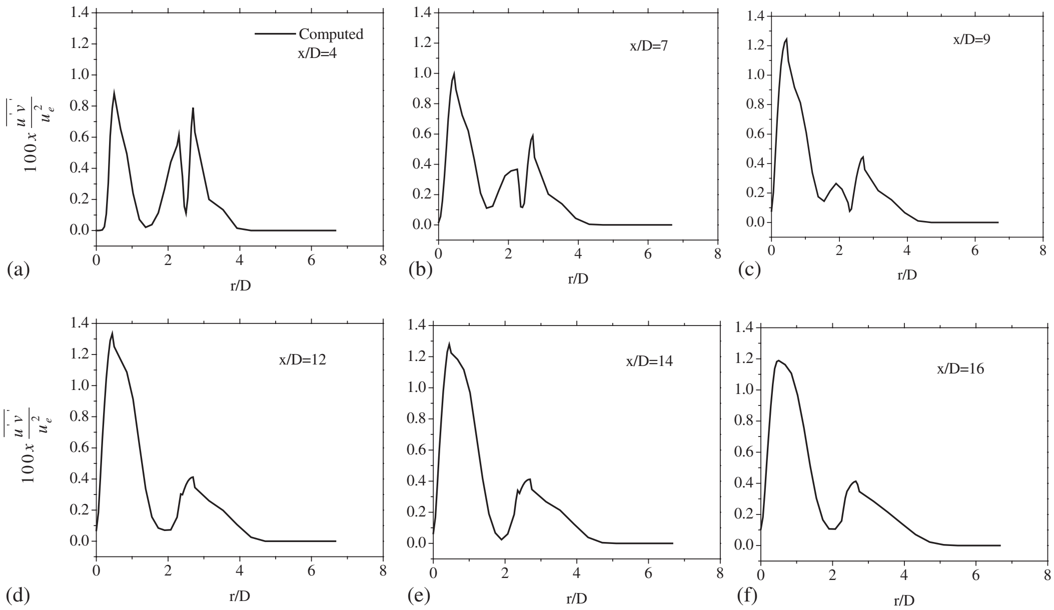

Figure 17. Variation of Reynolds shear stress for unequal jets ($S/D = 2.5$, $d/D = 0.5$).

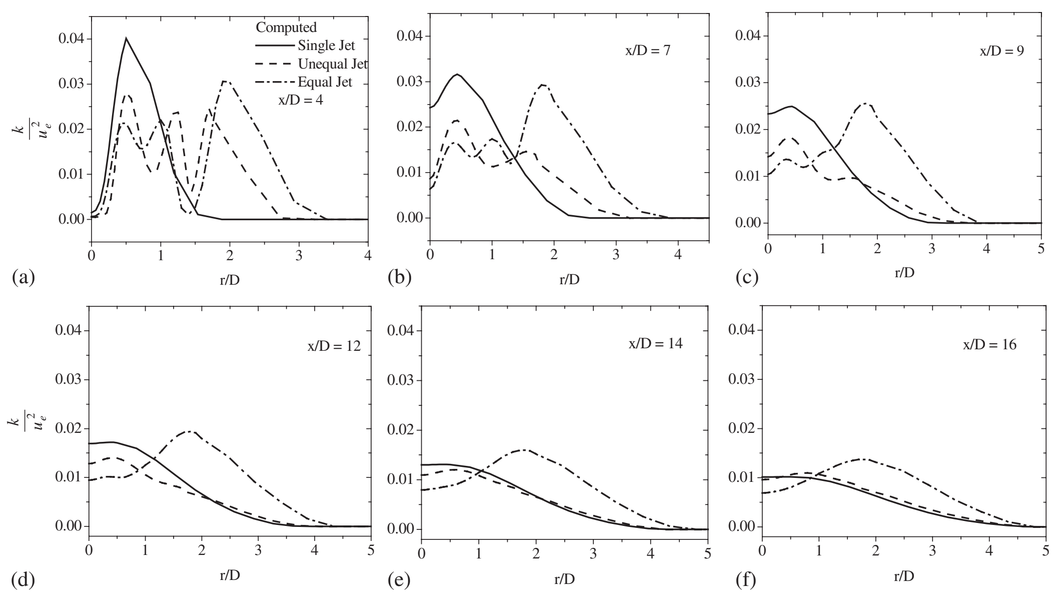

Figure 18. Comparison of turbulent kinetic energy of unequal five-jets ($S/D = 1.5$, $d/D = 0.5$) with that of a single jet.

APPENDIX A. NOMENCLATURE

d	peripheral jet diameter
D	equivalent jet diameter
f	frequency
p_o	stagnation pressure
p	static pressure
p_∞	ambient pressure
$Y_{0.5}$	half width of the jet
Q_e	volume flux at nozzle exit
St	Strouhal number
T	static temperature
T_o	stagnation temperature
U	velocity component along X-axis
U_c	axial velocity component
U_e	axial velocity at nozzle exit
V	velocity component along Y-axis
θ_e	momentum thickness of the boundary layer at the exit section
μ	viscosity
ρ	density
τ	viscous stress tensor

REFERENCES

1. Wygnanski I, Fiedler HE. Some measurements in the self-preserving jet. *Journal of Fluid Mechanics* 1969; **38**:577–612.
2. Donaldson CD, Snedeker R. A Study of free jet impingement. Part 1: Mean properties of free and impinging jets. *Journal of Fluid Mechanics* 1971; **45**:281–319.
3. Crow SC, Champagne FH. Orderly structure in jet turbulence. *Journal of Fluid Mechanics* 1971; **48**:547–591.
4. Zaman KBMQ, Hussain AKMF. Turbulence suppression in free shear flows by controlled excitation. *Journal of Fluid Mechanics* 1981; **103**:133–159.
5. Gutmark EJ, Grinstein FF. Flow control with non-circular jets. *Annual Review of Fluid Mechanics* 1999; **31**:239–272.
6. Elbanna H, Sabbagh JA. Interaction of two non-equal plane parallel jets. *American Institute of Aeronautics and Astronautics Journal* 1987; **25**(1):12–13.
7. Ho CM, Gutmark EJ. Vortex induction and mass entrainment in a small aspect ratio elliptic jet. *Journal of Fluid Mechanics* 1987; **179**:383–405.
8. Hussain AKMF, Hussain HS. Elliptic jets. Part 1: Characteristics of excited and unexcited jets. *Journal of Fluid Mechanics* 1989; **208**:257–320.
9. Gutmark EJ, Grinstein FF. Flow control with non-circular jets. *Annual Review of Fluid Mechanics* 1999; **31**:239–272.
10. Zaman KBMQ. Axis switching and spreading of an asymmetric jet: The role of coherent structure dynamics. *Journal of Fluid Mechanics* 1996; **316**:1–27.
11. Zaman KBMQ. Spreading characteristics of compressible jets from nozzles of various geometries. *Journal of Fluid Mechanics* 1999; **383**:197–228.
12. Verma SB, Rathakrishnan E. Flow and noise characteristics of notched elliptic orifice jets. *Journal of Fluids Engineering* Transactions of the ASME 1999; **121**:690–693.
13. Lau JC, Morris PJ, Fisher MJ. Measurements in subsonic and supersonic free jets using a laser velocimeter. *Journal of Fluid Mechanics* 1979; **93**(1):Part 1, 1–27.
14. Krothapalli A, Baganoff D, Karamacheti K. Development and structure of a rectangular jet in a multiple jet configuration. *American Institute of Aeronautics and Astronautics Journal* 1980; **18**(8):945–950.
15. Raghunathan, Reid IM. A study of Multiple jets. *American Institute of Aeronautics and Astronautics Journal* 1981; **19**(1):124–127.
16. Vijayakumar S. Experimental and numerical studies on the interaction between unequal supersonic free jets. *M.S. Thesis*, Indian Institute of Technology, Madras, 2000.

